

The Morphology and Defect Characteristics of Vertically Pulled MgAl_2O_4 Single Crystals

B. COCKAYNE, M. CHESSWAS, P. J. BORN, J. D. FILBY
Royal Radar Research Establishment, Malvern, Worcs, UK

Received 7 October, and in revised form 21 November

Optical, etch pit and X-ray topographic studies of magnesium aluminate spinel (MgAl_2O_4) have shown that undoped single crystals vertically pulled from stoichiometric melts can exhibit a high degree of crystalline perfection. The principal defect is strain arising from the formation of $\{111\}$ facets on the solid/liquid interface. This effect is inhibited by suitable control of interface shape, but is greatly enhanced by the presence of chromium which segregates non-uniformly between the facets and the bulk of the crystal. Chromium also causes strain in the impurity-rich bands corresponding to growth striations.

1. Introduction

Single crystal spinel, MgAl_2O_4 , is of interest as an insulating substrate material for the epitaxial deposition of both silicon [1] and gallium arsenide [2], and is of potential use in passive ultrasonic delay line applications [3]. For these purposes, stoichiometric single crystals with a high degree of crystalline perfection are required. Traditionally, spinel crystals have been grown by flame-fusion techniques [4], and are generally rich in Al_2O_3 . This excess of one component often impairs crystalline perfection by precipitation along dislocation low-angle boundaries of a phase mechanically harder than the matrix. Stoichiometric crystals have been produced by flux techniques [5], but such crystals are usually too small for device requirements. More recently, two of the present authors [6] described a technique which allows single crystals to be vertically pulled from a stoichiometric spinel melt, and in the present paper, the characteristic defects and the morphology of such crystals are described, together with some effects resulting from doping crystals with chromium.

2. Crystal Growth

The crystals described here were all grown using the apparatus and technique described in an earlier publication [6]. Iridium crucibles of two different sizes, namely 3.75 cm diameter \times 3.75 cm height and 5.25 cm diameter \times 10 cm height, were used to contain the melt. Typical sizes of

crystals grown were 1 cm diameter \times 5 cm long from the small crucible, and 2.5 to 3.0 cm diameter \times 9.0 cm long from the larger one. The spinel melts were prepared from the component powders, MgO and Al_2O_3 , which were supplied as Optran grade material by British Drug Houses Ltd.

The crystals were grown on $\langle 100 \rangle$, $\langle 110 \rangle$, or $\langle 111 \rangle$ seeds at pull and crystal rotation rates within the ranges 5 to 20 mm/h and 0 to 150 rev/min respectively.

3. Crystal Morphology

The standard Laue X-ray back reflection technique was used to determine the characteristic facets developed by spinel single crystals grown on axes corresponding to the three principal low index orientations. $\langle 100 \rangle$ axis crystals are square in section, the four sides of the square being $\{100\}$ planes. $\langle 110 \rangle$ axis crystals have a hexagonal section, two opposite sides being equivalent to $\{100\}$ planes whilst the remainder are $\{111\}$ planes. $\langle 111 \rangle$ axis crystals develop a triangular section, the three sides of which are $\{211\}$ planes. All these facets develop parallel to the growth axis.

Facets of the type $\{111\}$ have also been observed on the decanted solid/liquid interface. These facets extend over those areas of the interface which are approximately parallel to $\{111\}$ planes, and as a consequence, their size and position on the interface are markedly dependent

upon the interface shape. At normal rotation rates (20 to 50 rev/min), 1 cm diameter crystals grown from the small crucible exhibit interfaces which are markedly convex towards the melt, being approximately conical in shape with the side of the cone intersecting the growth axis at approximately 40° . As $\{111\}$ planes make angles of 35° , 0° or 55° , and 20° or 90° with the $\langle 100 \rangle$, $\langle 110 \rangle$ and $\langle 111 \rangle$ directions respectively, the interface facets are most readily observed in $\langle 100 \rangle$ axis crystals. In this case four facets are observed generally near to the centre of the interface. Two facets form on $\langle 110 \rangle$ axis crystals, but these are usually observed only when the interface is slightly more convex towards the melt than quoted above (i.e. the interface intersects the growth axis at approximately 50 to 55°). Such a condition can be induced either by decreasing the crystal diameter with respect to the crucible diameter, or by decreasing the crystal rotation speed. No facets have been observed on $\langle 111 \rangle$ axis crystals. The formation of facets on the interface is completely inhibited by rotating the crystal at high speed (approximately 100 rev/min) in the small crucible, or by growing the crystal from the large crucible containing less than 50 vol % of melt. Both these conditions produce an interface which is only slightly convex towards the melt (the interface intersects the growth axis at approximately 85°) a situation which is unfavourable for $\{111\}$ facet development in $\langle 100 \rangle$ or $\langle 110 \rangle$ axis crystals. No $\langle 111 \rangle$ axis crystals have been grown under these conditions but in such circumstances it should be possible for a single $\{111\}$ facet to develop across the entire interface.

4. Chromium Doping

4.1. Facet Effect

When crystals are grown from melts containing chromium added in the form of Cr_2O_3 , under conditions where $\{111\}$ type facets form on the solid/liquid interface, the chromium segregates non-uniformly between the faceted and non-faceted region. The autoradiograph of fig. 1 was obtained using Cr^{51} as a radioactive tracer and shows two dark areas in the centre of a $\langle 110 \rangle$ axis crystal grown from a melt containing 0.05 at. % Cr. These areas correspond to $\{111\}$ facets and are deficient in chromium with respect to the bulk of the crystal. This difference in chromium concentration causes strain in the faceted region, as shown for a $\langle 100 \rangle$ axis crystal in the photomicrograph of fig. 2. The stresses

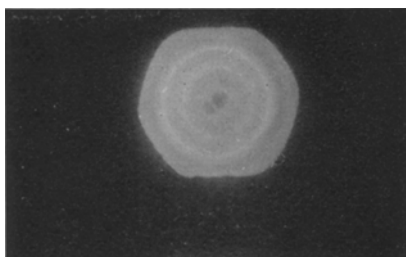


Figure 1 Autoradiograph of a $\langle 110 \rangle$ axis spinel crystal doped with 0.05 at. % Cr^{51} . Transverse section showing growth striations and facet effect ($\times 2$).

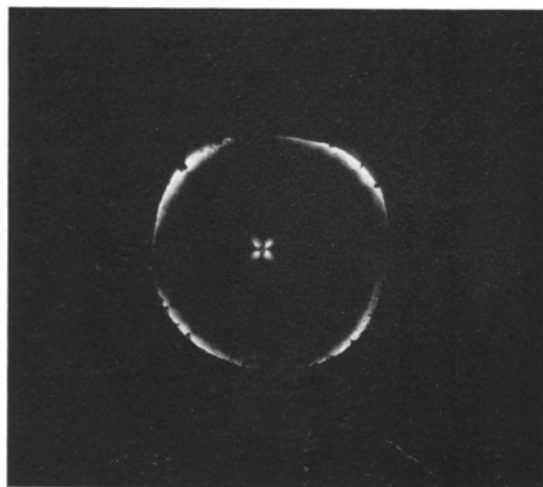


Figure 2 Transverse section of a $\langle 100 \rangle$ axis spinel crystal containing 0.05 at. % Cr viewed between crossed polaroids ($\times 3$).

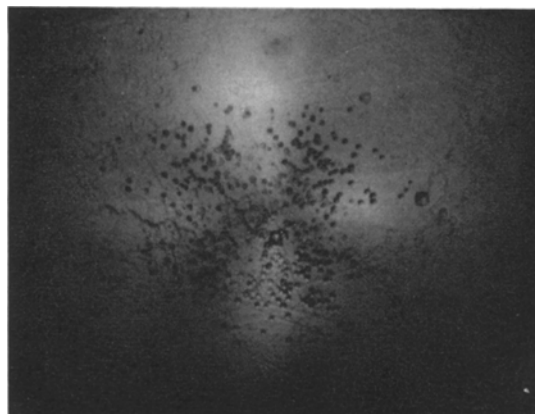


Figure 3 Dislocation etch pit pattern in the strained region of the crystal shown in fig. 2. Viewed between crossed polaroids ($\times 68$).

developed within the faceted region appear to exceed the yield point of spinel at some point during growth, since dislocations are generated in this region, as depicted by the etch pit pattern of fig. 3. The dislocations must form above 1550° C as spinel is non-ductile below this temperature [7]. No etch pits are observed in the central region of those crystals which are either undoped or free from facets.

4.2. Growth Striations

In addition to non-uniform segregation due to the facet effect, fig. 1 exhibits variations of chromium concentration occurring in a concentric ring pattern. Fig. 4 shows that such rings represent growth striations viewed in a direction perpendicular to the growth axis; such striations

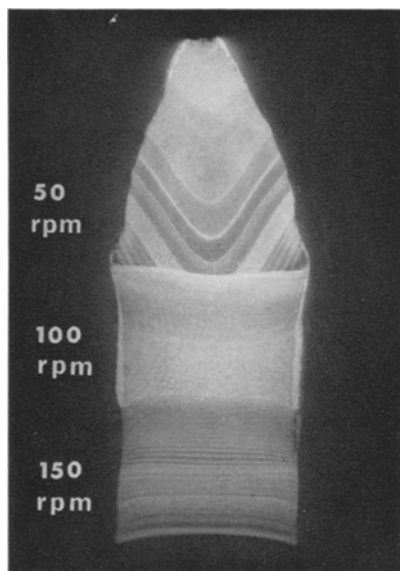


Figure 4 Autoradiograph of a longitudinal section of a $\langle 110 \rangle$ axis spinel crystal doped with 0.05 at. % to Cr^{51} showing the effect of crystal rotation upon the growth striations and interface shape ($\times 1.8$).

are characteristic of vertically pulled crystals and delineate the shape of the solid/liquid interface. In the case illustrated by fig. 1, the crystal was grown at 50 rev/min, and the solid/liquid interface was conical in shape. The autoradiograph of fig. 4 shows the flattening of the interface which occurs as the crystal rotation speed is increased.

The growth striations represent changes in chromium concentration and do not differ

significantly in appearance from those previously reported in other oxide crystals [8, 9]. They are generally attributed to temperature fluctuations which arise from unstable thermal convection, and which modulate the growth rate of the crystal thereby producing a corresponding change in the distribution coefficient of the added impurity.

4.3. Distribution Coefficient

The bulk distribution coefficient of chromium in spinel has been determined according to the equation

$$C_s = C_0 k (1 - g)^{k-1}$$

where k is the distribution coefficient, C_0 is the original chromium concentration in the melt and C_s is the concentration of chromium in the solid at the point where fraction g of the melt has solidified. C_s was measured by scintillation counting of Cr^{51} incorporated in successive transverse slices of equal thickness cut from the full length of $\langle 110 \rangle$ axis crystals grown at a pulling rate of 8 mm/h and a rotation rate of 50 rev/min. Crystals were grown from melts containing 0.05 and 0.10 at. % Cr^{51} for this investigation. The results presented in table I, show that the distribution coefficient of Cr in spinel is considerably greater than unity and further suggest that its value is slightly concentration dependent.

TABLE I

At. % Cr^{51} in melt	% of melt converted to crystal	Distribution coefficient, k
0.05	59	2.6 ± 0.1
0.10	36	2.4 ± 0.1

5. Dislocations

Apart from the dislocations introduced by faceting in doped crystals, the dislocation density as revealed by etch pits is low, and is typically in the region 10^2 to 10^3 per cm^2 . Low-angle boundary arrays are not observed and most of the dislocations occur in slip bands lying along $\langle 110 \rangle$ directions near the periphery of the crystals, as shown in fig. 5. These bands lie in the strained regions which may be seen around the edge of the crystals shown in fig. 2. This peripheral region of strain is least evident in crystals cooled slowly to room temperature and thus appears to be related to the steeper temperature gradients and

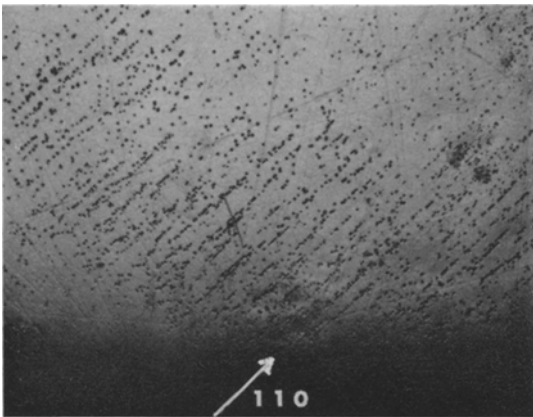


Figure 5 Dislocation etch pit pattern of the strained outer region of the crystal shown in fig. 2 ($\times 38$).

consequently higher thermal stresses to which the crystal edge is subjected with respect to the centre. It is observed in both pure crystals and those doped with chromium, but the strain level is enhanced in the latter case.

In order to remove work damage introduced by mechanical polishing, the specimens for etch pit studies were chemically polished in a 2:1 PbF_2/PbO mixture at 700°C for 20 to 30 min or in phosphoric acid at 300°C for 3 to 5 h. Molten KHSO_4 at 750°C was found to be a suitable dislocation etchant on $\{111\}$ and $\{100\}$ planes but molten Li_2WO_4 at 750°C was more effective on $\{110\}$ planes.

6. Stoichiometry

Crystals can be grown from stoichiometric melts at rates up to 20 mm/h without the onset of void formation, which occurs in oxides because of constitutional supercooling due to the rejection of either solid or gaseous impurity at the growing interface [10]. However, the deliberate addition to the melt of 2 mol % excess of either Al_2O_3 or MgO readily initiates void structures at comparable growth rates. The crystals grown from stoichiometric melts must thus be near to the stoichiometric composition and hence the normally volatile MgO is not readily lost from a stoichiometric melt of spinel. This is further confirmed by the measured lattice spacing of $8.0857 \pm 0.0005 \text{ \AA}$, determined by an X-ray powder diffraction technique using an 11.4 cm Debye-Scherrer camera and $\text{Cu K}\alpha$ radiation. This measurement is in good agreement with values of 8.085 and 8.089 already reported for stoichiometric spinel [11, 12].

7. X-ray Diffraction Topography

In order to study strain distribution in greater detail, vertically pulled spinel crystals have been examined by the X-ray diffraction topography technique developed by Lang [13]. For these studies 0.5 mm thick samples were cut from the crystals, mechanically polished to 0.4 mm and subsequently chemically polished to a thickness of approximately 0.25 mm in the manner already described (section 5). The topographs were recorded using $\text{Ag K}\alpha$ radiation on Ilford nuclear plates, type L4, with 50 mm thick emulsion.

The general findings of the optical studies are confirmed by the X-ray topographic investigation in that faceted regions and the edges of the crystals are strained. These can be observed in the topographs of figs. 6 and 7, where strained regions appear as light areas.

The topographs also reveal several additional features of interest. For instance, a comparison of fig. 6 (220 reflection), with the autoradiograph of an adjacent section of crystal (fig. 5) shows that the growth striations, which are chromium rich relative to the matrix, cause strain bands within the crystal which increase in intensity with increasing chromium concentration. Furthermore, fig. 6 reveals that highly stressed regions are present in sections of the crystal where the rotation rate has been changed rapidly and melting back has occurred. The strain from the partial facetting which has occurred in the portion grown at 50 rev/min has spread into the part of the crystal grown subsequently at a higher rotation rate. This strain extends out towards the edge of the crystal approximately along a $\langle 111 \rangle$ direction. An $\{002\}$ reflection topograph of the same crystal section as fig. 6 revealed only the growth striations in the regions of crystal grown at 50 rev/min. This confirms the planar nature of the striations in the regions grown at higher rotation rates and is consistent with them lying along $\{110\}$ planes perpendicular to both the $\langle 110 \rangle$ growth direction and the $\{002\}$ reflecting planes.

Optical interference techniques and the dislocation etch pit studies show the undoped spinel crystals to possess a high degree of crystalline perfection. This is generally confirmed by the X-ray diffraction topographs but the latter do show two features not observable by the other techniques. One is the existence of four strained regions in $\langle 100 \rangle$ axis crystals, marked A in fig. 7a (taken using $02\bar{2}$ reflection) which

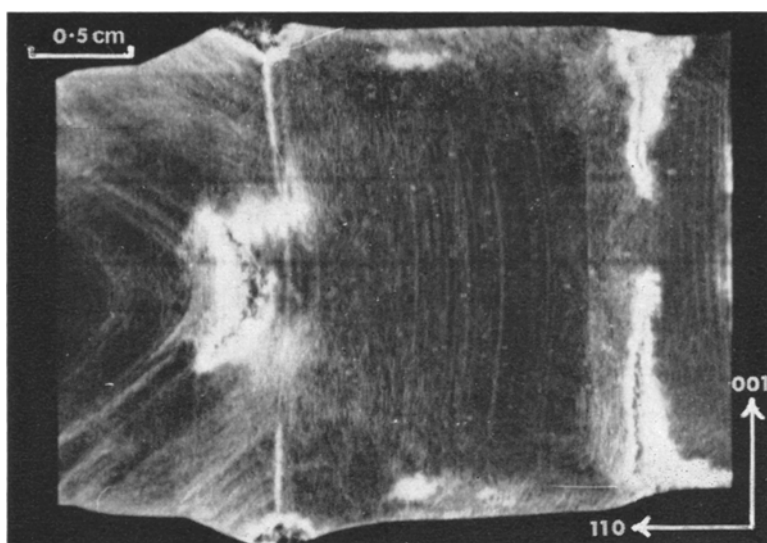


Figure 6 X-ray topograph (220 reflection) of a longitudinal (110) section of a $\langle 110 \rangle$ axis Cr-doped spinel crystal.

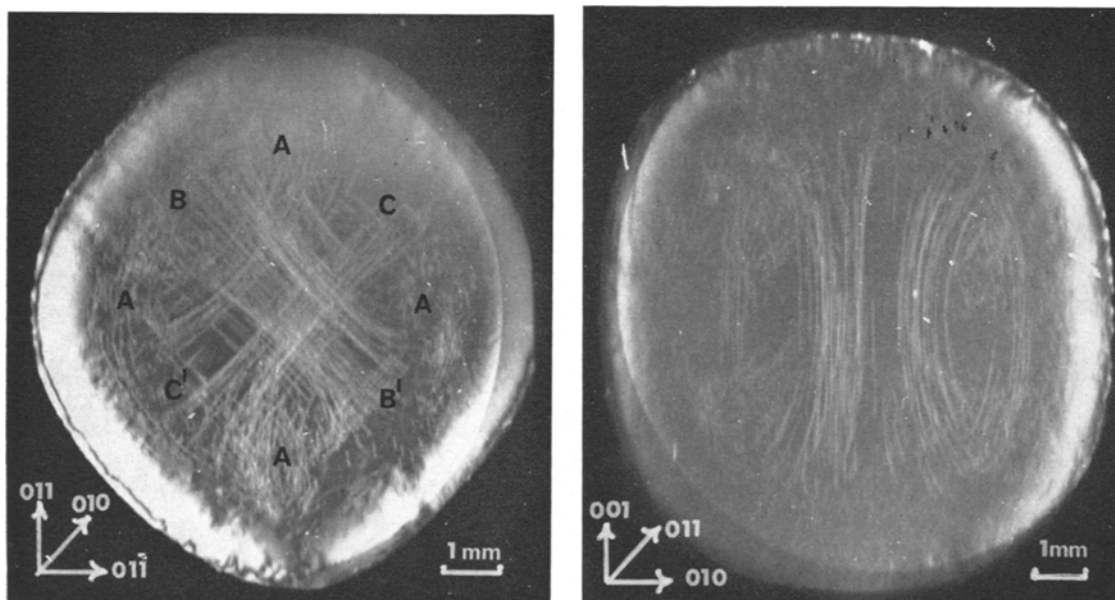


Figure 7 X-ray topographs of (a) $02\bar{2}$ reflection and (b) 020 reflection of a (100) transverse section from a $\langle 100 \rangle$ axis undoped spinel crystal.

corresponds to $\{111\}$ poles and to the position of the $\{111\}$ facet development on the interface of this particular crystal. The strain in these regions is presumably at a very low level since it is not observable between crossed polaroids. The second feature is the two sets of strain bands intersecting each other at right-angles in the centre of the crystal. The two features are related. This is not readily apparent from fig. 7a but

fig. 7b shows a topograph obtained using the 020 reflection which represents a clockwise rotation of the sample of 45° . In fig. 7b, the diagonal strain bands (B-B') can be seen as two independent loops with a $\{111\}$ strained region at the end of each loop. A further 90° rotation of the sample produced a similar pair of loops responsible for the strain bands C-C'.

Topographs taken of crystals sectioned paral-

lel to the growth direction confirm that the outer skin of strained material is consistent with dislocations lying on a plane parallel to the growth direction as observed in the etch pit studies. The topograph studies also confirm that, in addition to causing strain in the faceted regions, the presence of chromium also raises the general level of strain with the crystals.

8. Conclusions

The strained faceted regions observed in Cr-doped spinel are similar to those observed in other high melting point oxides such as the rare-earth aluminium garnets [9]. However, unlike the garnets, the facets in spinel do not cause macroscopically observable strain in undoped material. Nevertheless, the more strain sensitive technique of X-ray diffraction topography shows that the facets do cause a certain amount of strain even in the absence of chromium. Hence, for devices using spinel where the avoidance of small lattice strains is important, it is obviously preferable to grow the crystals under the conditions specified to avoid facet formation i.e. by using a suitable combination of growth orientation and interface shape. The strained region around the crystal edge is relatively unimportant from a device viewpoint as it is generally removed during the cutting and polishing of specimens in order to meet shape and size requirements.

Acknowledgement

This paper is published by permission of The Controller, HMSO.

References

1. P. H. ROBINSON and D. J. DUMIN, *J. Electrochem. Soc.* **115** (1968) 75.
2. H. M. MANASEVIT, *Appl. Phys. Lett.* **4** (1968) 156.
3. M. F. LEWIS and E. PATTERSON, *J. Appl. Phys.* **39** (1968) 3420.
4. R. H. ARLETT, *J. Amer. Ceram. Soc.* **45** (1962) 523.
5. R. C. LINARES, *J. Appl. Phys.* **33** (1962) 1747.
6. B. COCKAYNE and M. CHESSWAS, *J. Materials Sci.* **2** (1967) 498.
7. M. H. LEWIS, *Phil. Mag.* **17** (1968) 481.
8. B. COCKAYNE and M. P. GATES, *J. Materials Sci.* **2** (1967) 118.
9. J. BASTERFIELD, M. J. PRESCOTT, and B. COCKAYNE, *ibid* **3** (1968) 33.
10. W. BARDSLEY and B. COCKAYNE, "Crystal Growth" Proceedings of International Conference on Crystal Growth, Boston, 1966 (Pergamon Press, Oxford, 1967) p. 109.
11. R. H. ARLETT and MURRAY ROBBINS, *J. Amer. Ceram. Soc.* **50** (1967) 273.
12. J. G. GRABMAIER and B. CHR. WATSON, *ibid* **51** (1968) 355.
13. A. R. LANG, *Acta Cryst.* **12** (1959) 249.